Copolymer-MnO2 nanocomposites for the adsorptive removal of organic pollutants from water

Arun Viswan Kalarikkandy
Amrita Vishwa Vidyapeetham Amrita School of Engineering
Nirmal Sree
Amrita Vishwa Vidyapeetham Amrita School of Engineering
Sanjay Ravichandran
Amrita Vishwa Vidyapeetham Amrita School of Engineering
Gangadharan Dheenadayalan (dharan.ganga@gmail.com)
Amrita School of Engineering Coimbatore Campus https://orcid.org/0000-0003-3965-977X

Research Article

Keywords: Copolymer-MnO2 nanocomposite, adsorption, organic pollutants, desorption, wastewater

Posted Date: April 22nd, 2022

DOI: https://doi.org/10.21203/rs.3.rs-1508447/v1

Version of Record: A version of this preprint was published at Environmental Science and Pollution Research on July 23rd, 2022. See the published version at https://doi.org/10.1007/s11356-022-22137-2.

Abstract

The copolymer beads prepared by suspension polymerization were decorated with MnO_2 nanoparticles and successfully implemented for the efficient removal of toxic organic contaminants from water. Copolymer-MnO_2 nanocomposite was further analysed using XRD, SEM, and optical microscope. The SEM images showed the surface characteristics of MnO_2 nanoparticles on copolymer beads. The efficiency of the copolymer-MnO_2 nanocomposite for the removal of model pollutant methylene blue and rhodamine B is then analysed by changing the concentration of pollutant. The results obtained exhibited 18.45 mg/g for methylene blue adsorption and 3.125 mg/g for rhodamine B. The adsorption equilibrium results were fitted to Langmuir adsorption isotherm for both methylene blue and rhodamine B adsorption. The desorption studies were performed for five consecutive cycles and material was showing good regenerating capacity towards both organic pollutants. The obtained results show that copolymer-MnO_2 nanocomposite is an efficient material for the removal of organic contaminants from wastewater.

1. Introduction

Water pollution is a worldwide issue that affects the human population around the world. Reliably, a lot of wastewater is created by industrial, horticultural and household activities and are stored in the land or water receptors (Reddy et al. 2022) (Chowdhary et al. 2020). The polluted water can cause harmful effects on aquatic as well as terrestrial life (Nagarajan &Venkatanarasimhan 2019) (Nagarajan &Venkatanarasimhan 2020). There is an increasing number of toxic pollutants in today's environment, requiring new materials to remove them. The occurrence of toxic dyes in water is one among them and they can slowly lead to serious health problems. Wastewater or effluents need to be treated in order to be reused or disposed without harming the environment or human health.

Organic dyes, Methylene blue (MB) and rhodamine B (RhB) are widely used in the textile industry and can cause various health issues when present in water (Karthik et al. 2018). Exposure to these dyes can lead to skin issues, eye problems, etc. (Tang et al. 2018). Various techniques such as coagulation, chemical oxidation, membrane filtration, adsorption etc. have been used for the removal of dyes from water (Crini &Lichtfouse 2019). In which adsorption obtained wide attention due to its low cost and higher efficiency (Bonilla-Petriciolet et al. 2017). Researchers prepared various adsorbent materials for the removal of such toxic dyes from water. Activated carbon (Xue et al. 2022) (Han et al. 2020), graphene oxide(Benjwal et al. 2015) (Huang et al. 2019), Fe_3O_4 (Zhang et al. 2013) are various adsorbent materials reported for the removal of MB. Sharma et al (Sharma et al. 2018) synthesized agrobacterium fabrum biomass along with iron oxide nanoparticles for the removal of MB and the material was showing a good regenerating capacity for four consecutive cycles. Similarly, various adsorbent materials such as polymer (KK &Gangadharan 2018), activated carbon (Zhang et al. 2021), silica (Joshiba et al. 2021), MOF (Liu et al. 2016), nanoparticles (Hund-Rinke &Simon 2006), nanocomposites(Skiba &Vorobyova 2020) etc. are used for the removal of contaminants (Elias et al. 2021) from water. Polymers and nanomaterials are among the newest emerging materials used to remove contaminants from water. Nanocomposites made of polymer materials have gained wide attention for their performance and ease of separation from contaminant solutions (Beyene &Ambaye 2019). Adding nanoparticles to polymers can improve their efficiency (Khodakarami &Bagheri 2021).

MnO_2 is considered an efficient nanomaterial for wide range of applications. It is widely used in batteries (Liu et al. 2019), supercapacitors (Kubra et al. 2020), sensors (Cogal et al. 2021), and wastewater purification processes (KK &Gangadharan 2022). Different materials were modified with MnO_2 nanoparticles to improve the adsorption efficiency (Cuong et al. 2021) (Verma et al. 2021). Dong et al (Dong et al. 2010) synthesized a MnO_2 loaded resin for the simultaneous adsorption of lead and cadmium from the aqueous solution. Here, surface complexation plays a vital role in the adsorption of lead and cadmium on MnO_2-loaded resin. Similarly, various materials have been prepared using MnO_2 as a component. The separation of MnO_2 nanoparticle from adsorbate solution is a challenge for researchers. To overcome this, copolymer beads can incorporate with MnO_2 material for the easy separation of material from aqueous solution as well as to improve the adsorption capacity of material towards organic pollutants (Gangadharan et al. 2013). Column studies can also be performed by using copolymer beads. Nhat Ha et al (Nhat Ha et al. 2016) synthesized layered double hydroxide embedded polymer beads for the removal of arsenate ions via batch as well as column studies. The removal of contaminants via the column method is an advantage of using polymer beads-modified materials.

Herein, this research work focused on the synthesis, characterization and application of a copolymer-MnO_2 nanocomposite. The as synthesized copolymer-MnO_2 nanocomposite material was then analysed using powder XRD, SEM and optical microscope. The material is then equilibrated with organic pollutants to find the maximum adsorption capacity towards organic pollutant removal. As model pollutants, methylene blue and rhodamine B were used. Furthermore, the effect of contact time and concentration of pollutants on the material were studied. The regenerating capacity of the material was established by performing adsorption-desorption studies. The concentration studies were conducted by using a UV-Visible spectrophotometer.

2. Experimental

2.1. Materials

Manganese sulphate, potassium permanganate, methylene blue, and rhodamine B were obtained from Merk. Distilled water was used in all the experiments.

2.2. Preparation of copolymer beads

As previously reported, the preparation of copolymer beads was undertaken (Gangadharan et al. 2010). To a beaker containing 35 mL methacrylic acid add 5.4 mL of divinylbenzene followed by addition of 0.4 g of benzoyl peroxide dissolved in 12 mL toluene. To a preheated three-neck round bottom flask containing 2% starch solution as suspension medium, the monomeric mixture was gradually added at 70°C while the flask was preheated. Following the addition of the monomeric mixture, the temperature was raised to 80°C and maintained under a reflux condition for 5 hours. Physically decanting the solution finally separated the opaque white spheres from the solution.

2.3. Modification of copolymer-MnO_2 nanocomposite

2 g of synthesised copolymer beads were weighed and taken in a conical flask and treated with 200 mL of 0.1M $MnCl_2.4H_2O$ solution in a mechanical stirrer for 18 hours. Afterward, it was decanted and washed with deionised water to eliminate any excess Mn^{2+} ions adhering to the copolymer beads. Mn^{2+} ions loaded methacrylic acid copolymer beads were treated with 200 mL of 0.1M $KMnO_4$ solution in a mechanical stirrer for 18 hours. The

solution was then decanted and washed with deionized water to remove loosely adhering MnO_2 from the copolymer beads.

2.4. Copolymer-MnO_2 nanocomposite characterisation

The synthesized copolymer beads and copolymer-MnO_2 nanocomposite was analysed using OLYMBUS CH20i optical microscope. The cross section of copolymer-MnO_2 nanocomposite was analysed to determine the pattern of loading on the copolymer beads. SEM analysis was carried out to know the morphology of the MnO_2 loaded on the copolymer beads. An Empyrean range instrument with a Cu K□ target was used for X-ray diffraction experiments in a region of 2□ from 20° to 80°. UV-Visible spectroscopy was used to analyse the concentration of methylene blue (MB) and RhB in the water samples.

2.5. Adsorption studies of MB on copolymer-MnO_2 nanocomposite

200 mg of copolymer-MnO_2 nanocomposite were taken in 5 different stoppered conical flasks to which 50 mL of freshly prepared 5, 10, 15, 20 and 25 ppm methylene blue solutions were added respectively. They were kept for shaking in a mechanical stirrer for 10 hours and the solutions were tested for adsorption of different concentrations of methylene blue on copolymer-MnO_2 nanocomposite. All these studies were carried out at neutral pH 7.

2.6. Adsorption of RhB on copolymer-MnO_2 nanocomposite

The copolymer-MnO_2 nanocomposite were then used to remove the toxic dye RhB from aqueous solutions. A batch method was used to study adsorption. In a 250 ml stoppered flask, 200 mg of the copolymer-MnO_2 nanocomposite were equilibrated with 20 mL of RhB solution with a concentration ranging from 5 mg/L to 25 mg/L. The equilibration attained within 10 hours and the absorbance of the solution after adsorption is measured using UV-Visible spectrophotometer.

2.7. Desorption of MB from copolymer-MnO_2 nanocomposite

To examine the regenerating capacity of the copolymer-MnO_2 nanocomposite, the MB dye was desorbed from the copolymer-MnO_2 nanocomposite. 200 mg of the material was equilibrated with 50 mL of 5 mg/L of MB solution for 10 hours. The MB loaded material was then treated with 30 mL of ethanol to desorb the MB. The quantity of MB desorbed from the copolymer-MnO_2 nanocomposite was then estimated using UV-Visible spectrophotometer. The experiment was repeated five times to determine the regenerative capacity of copolymer-MnO_2 nanocomposite.

2.8. Desorption of RhB from copolymer-MnO_2 nanocomposite

200 mg of the copolymer-MnO_2 nanocomposite was equilibrated with 20 mL of 5 mg/L of RhB solution for 10 hours. 20 mL of 1M acetic acid was then added to the RhB-loaded copolymer-MnO_2 nanocomposite to desorb it. The amount of RhB absorbed onto copolymer-MnO_2 nanocomposite was then determined using a UV-visible spectrophotometer. Five cycles of the experiment were conducted to test the regenerating capacity of the material.

2.9. Scheme of work

The copolymer-MnO_2 nanocompositewere treated with MB and RhB solution. The contaminants were loaded on the beads via adsorption process. MnO_2 particles were observed both on the surface and interior core of the copolymer beads. Adsorption of MB dye onto the beads turns them green. Similarly, RhB dye was adsorbed onto the black coloured MnO_2 copolymer beads which turned red colour. The contaminants adsorbed on the surface were desorbed using ethanol and acetic acid solution. The MnO_2 loaded on the copolymer beads were removed using HCl solution.

3. Results And Discussion

3.1. Characterisation of copolymer-MnO_2 nanocomposite

3.1.1. Powder X-ray diffraction analysis of copolymer-MnO_2 nanocomposite

The presence of MnO_2 nanoparticles on the copolymer beads was determined using powder XRD analysis data. The peaks at two theta values 12.2, 36.4, 65.7 and 85.7 degrees which represent the MnO_2 nanoparticles on the polymer surface. The lattice planes corresponding to the given two theta values are (110), (400), (002), and (512). The powder XRD spectra was given in Fig. 2. The spectra were then compared with the standard ICDD data (02-0227).

3.1.2. SEM analysis of copolymer-MnO_2 nanocomposite

The analysis using scanning electron microscope was performed to study the distribution of MnO_2 surface morphology of the copolymer-MnO_2 nanocomposite. The SEM images of copolymer beads and copolymer-MnO_2 nanocomposite was given in Fig. 3. Figure 3a represent the copolymer beads without MnO_2 is spherical in shape. Figure 3b represent the MnO_2 particle on the polymer surface. The MnO_2 particle exhibited spherical shape and attached on the polymer surface. Figure 3c shows the MnO2 nanoparticles observed on the cross-sectional image of polymer beads. Nanoparticles conformed to be smaller than 100 nm in size. The Fig. 3d represent the EDX spectra of the copolymer-MnO_2 nanocomposite. This study showed the presence of Mn on copolymer beads.

3.1.3. Optical microscopic analysis of copolymer-MnO_2 nanocomposite

Copolymer beads and copolymer-MnO_2 nanocomposite were analysed using optical microscope which is given in Fig. 4. The copolymer beads prepared by suspension polymerization was shown in Fig. 4a. The colour remained white even after exchange of Mn^{2+} ions and turned into black colour after treating with $KMnO_4$ which is given in Fig. 4b and 4c respectively. On the optical microscope cross section image of the copolymer-MnO_2 nanocomposite, it can be seen that MnO_2 has formed on the surface as well as inside, as shown in Fig. 4d. This copolymer-MnO_2 nanocomposite was used to remove the organic pollutants from water.

3.2. Adsorption of MB and RhB on copolymer-MnO_2 nanocomposite

Contact time and adsorbate concentration influenced the adsorption of MB and RhB. Adsorption of MB on copolymer-MnO_2 nanocomposite at different time interval was studied to fix the equilibration time. 200 mg of the copolymer-MnO_2 nanocomposite was equilibrated with 50 mL of 5 mg/L MB solution. A UV-Visible spectrophotometer was used to measure the absorbance of the solution at each 1-hour interval. The time studies unveil that, 48% of the MB got adsorbed within 1 hour of equilibration and attained equilibrium within 9 hours. 98% of the MB was adsorbed on copolymer-MnO_2 nanocomposite after equilibration. The adsorption percentage in each time interval was graphically shown in Fig. 5a.

Likewise, the effect of contact time for RhB adsorption on copolymer-MnO_2 nanocomposite was studied. 200 mg of the copolymer-MnO_2 nanocomposite was equilibrated with 20 mL of 5 mg/L solution. The obtained data was graphically shown in Fig. 5b. The material was showing a good adsorption tendency towards RhB. Initially, 46% of the RhB was adsorbed on copolymer-MnO_2 nanocomposite within 1 hour and attained 96% adsorption after 10 hours of equilibration.

Batch adsorption data studies for MB was then performed to check the effect of adsorbate concentration on copolymer-MnO_2 nanocomposite. The MB solution with concentration ranging from 5 to 25 mg/L were used for the analysis. 200 mg of the adsorbent was equilibrated with 50 mL of each MB solution for 10 hours of equilibration. The results obtained from above studies showed that 98% of the adsorbate adsorbed on to the material from 5 mg/L solution. Adsorption percentage was decreased to 60% for 25 mg/L solution. The adsorption data was given in Fig. 5c.

Likewise, batch adsorption studies of RhB were performed using different concentration ranging from 5 to 25 mg/L. 200 mg of the adsorbent was equilibrated with 20 mL of each RhB solution for 10 hours of equilibration. The result obtained showed an adsorption efficiency of 96% for 5 mg/L RhB solution. Similarly, adsorption efficiency was 94%, 88%, 85% and 84% for 5, 10, 15, 20 and 25 mg/L respectively. The results of the adsorption data is shown in Fig. 5d.

3.3. Isotherm studies for MB and RhB adsorption on copolymer-MnO_2 nanocomposite

Adsorption isotherms have been studied to determine the type of adsorption in case of MB and RhB removal from water. The results obtained from the adsorption study were fitted to Langmuir and Freundlich isotherm models.

According to Langmuir adsorption isotherms, monolayer adsorption can only occur on

homogeneous sites. The linear formula of the Langmuir isotherm is given as;

$$\frac{1}{q_e} = \frac{1}{q_m} + \frac{1}{K_L q_m C_e}$$

……. 1

Where q_e (mg/g) is the quantity of MB or RhB loaded onto the copolymer-MnO_2 nanocomposite, q_m (mg/g) represents the maximum adsorption capacity of the copolymer-MnO_2 nanocomposite, C_e (mg/g) represents the concentration of the MB or RhB at equilibrium and K_L (L/mg) is the Langmuir constant. The values of q_m and K_L can be calculated from the plot $1/q_e$ vs $1/C_e$. The plot showed that the correlation coefficient reached its maximum value of 0.99. This material has a maximum adsorption capacity of 18.45 mg/g. The Langmuir adsorption

isotherm for MB is depicted in Fig. 6a. RhB also exhibits a maximum correlation coefficient of 0.98, and its maximum adsorption capacity is 3.125 mg/g. Figure 6c shows the isotherm plot for RhB. The data for the isotherms can be found in table 1.

We investigated the Freundlich adsorption isotherm on adsorbent for MB and RhB to investigate their surface energy distributions and modes of multilayer adsorption. Freundlich adsorption isotherm supports adsorption processes that occur on heterogeneous surfaces. The Freundlich adsorption isotherm equation is;

$$logq_e = \log K_f + \frac{1}{n} logC_e$$

…… 2

An analysis of the Freundlich plot was performed by plotting log C_e versus log q_e values. The value of 1/n can be obtained from the graph. 1/n was observed between 0.2 and 0.8, indicating that the copolymer-MnO_2 nanocomposite was a good adsorbent for the removal of MB and RhB. As shown in Fig. 6b, the correlation coefficient reaches a maximum value of 0.75. The Freundlich plot for RhB is shown in Fig. 6d and the correlation coefficient was found to be 0.91. Table 1 gives the values obtained from the graph.

Isotherm Models	MB	RhB
Langmuir	q_m = 18.45 mg/g	q_m= 3.125 mg/g
	K_L= 0.204 L/mg	K_L=0.651 L/mg
	R^2 = 0.99	R^2 = 0.98
Freundlich	n = 4.54	n = 4.23
	K_f = 2.5	K_f = 5.57
	R^2 = 0.75	R^2 = 0.86

The correlation coefficient values of Langmuir and Freundlich adsorption isotherm were provided in table 1. The results showed that, adsorption of dyes on copolymer-MnO_2 nanocomposite fit for the Langmuir isotherm model. In comparison with the Langmuir model, the Freundlich adsorption isotherm had a low correlation coefficient value.

3.4. Desorption of MB from copolymer-MnO_2 nanocomposite

The MB loaded on the copolymer-MnO_2 nanocomposite was then desorbed with ethanol solution. 200 mg of the material was treated with 50 mL of 5 mg/L of MB solution for 10 hours. The MB loaded material was then treated with 30 mL of ethanol to desorb the MB. The experiment was continued for another five cycles to check the regenerating capacity of the copolymer-MnO_2 nanocomposite. The obtained results showed 98% adsorption efficiency and 95% desorption efficiency on the first cycle. It was showing 92% adsorption efficiency and 80% desorption on 5th cycle. The copolymer-MnO_2 nanocomposite was showing good regenerating capacity towards the removal of MB from water. The experimental results were graphically shown in Fig. 7a.

3.5. Desorption of RhB from copolymer-MnO_2 nanocomposite

The RhB adsorbed on the copolymer-MnO_2 nanocomposite was then desorbed using acetic acid solution. 200 mg of the material was equilibrated with 20 mL of 5 mg/L of RhB solution for 10 hours. The RhB loaded material was then treated with 1M acetic acid to desorb the RhB. A UV-Visible spectrophotometer was then used to estimate the amount of RhB desorbed from the sample. To determine the regenerative capacity of the material, the experiment was repeated five times. The obtained results showed 96% adsorption efficiency and 95% desorption efficiency on the first cycle. It was showing 88% adsorption efficiency and 85% desorption on 5th cycle. The copolymer-MnO_2 nanocomposite exhibited good regenerating capacity towards the removal of RhB from water. The experimental results were graphically shown in Fig. 7a.

Name of adsorbent	*MB Adsorption capacity(mg/g)*	*Reference*	*Name of adsorbent*	*RhB Adsorption capacity(mg/g)*	*Reference*
Fe/Cr hydroxide	22.8	(Namasivayam &Sumithra 2005)	3D layered double hydroxide	49.6	(Zhu et al. 2020)
Graphene oxide	188.68	(Li et al. 2013)	Hypercrosslinked polymeric adsorbent	25–55	(Huang et al. 2008)
Clay	6.3	(Gürses et al. 2004)	Kaolinite	46.08	(Khan et al. 2012)
Fly ash	5.57	(Kumar et al. 2005)	Surfactant-modified coconut coir pith	14.9	(Sureshkumar &Namasivayam 2008)
Glass fiber	2.24	(Chakrabarti &Dutta 2005)	Fly ash	10.0	(Chang et al. 2009)
Activated Rosa canina seeds	47	(Gürses et al. 2006)	Hypercross-linked polymeric adsorbent	2.1	(Huang et al. 2008)
pods of Caesalpinia echinata	288	(Georgin et al. 2021)			

4. Conclusion

In this study, we prepared methacrylic acid-divinylbenzene polymer beads via suspension polymerization were decorated with MnO_2 nanoparticles and successfully implemented for the efficient removal of toxic organic contaminants from water. Copolymer-MnO_2 nanocomposite was studied for the removal MB and RhB via adsorption. Copolymer-MnO_2 nanocomposite exhibited an adsorption capacity of 18.45 mg/g and 3.125 mg/L towards MB and RhB respectively. The Langmuir adsorption model was found to be the best fit model for the adsorption of MB and RhB on copolymer-MnO_2 nanocomposite. Desorption studies showed good regenerating capacity for copolymer-MnO_2 nanocomposite in five consecutive cycles for MB and RhB. The copolymer-MnO_2 nanocomposite showed 98% adsorption efficiency and 95% desorption towards MB on first cycle. Copolymer-MnO_2 nanocomposite showed 96% adsorption and 95% desorption efficiency towards RhB on first cycle. To conclude, the

copolymer-MnO_2 nanocomposite can be used as a good adsorbent material towards the removal of organic pollutants from water.

Declarations

Data Availability

The datasets generated and/or analyzed during the current study are not publicly available but are available from the corresponding author on reasonable request.

Acknowledgement

This study was funded by Amrita School of Engineering, Coimbatore, India; via internally funded research project (IFRP), Project number [AMRITA/IFRP-24/2014-2015/05].

Author contribution

Arun Viswan K K - Execution of work, characterization, validation, investigation, writing—original draft,

Nirmal Sree, - execution of adsorption studies.

Sanjay R – performed desorption studies and regeneration studies.

D.Gangadharan – correction and review, editing manuscript, conceptualization of work, result interpretation.

Funding - Internally funded research project (IFRP), Project number [AMRITA/IFRP-24/2014-2015/05]

Ethics approval - Not applicable.

Consent to participate - Not applicable.

Consent for publication - Not applicable.

Competing interests - The authors declare no competing interests.

References

1. Benjwal P, Kumar M, Chamoli P, Kar KK (2015) Enhanced photocatalytic degradation of methylene blue and adsorption of arsenic (iii) by reduced graphene oxide (rGO)–metal oxide (TiO 2/Fe 3 O 4) based nanocomposites. RSC Adv 5:73249–73260
2. Beyene HD, Ambaye TG (2019) Application of sustainable nanocomposites for water purification process, Sustainable Polymer Composites and Nanocomposites. Springer, pp 387–412
3. Bonilla-Petriciolet A, Mendoza-Castillo DI, Reynel-Ávila HE (2017) Adsorption processes for water treatment and purification. Springer, p 256
4. Chakrabarti S, Dutta BK (2005) On the adsorption and diffusion of methylene blue in glass fibers. J Colloid Interface Sci 286:807–811
5. Chang S-H, Wang K-S, Li H-C, Wey M-Y, Chou J-D (2009) Enhancement of Rhodamine B removal by low-cost fly ash sorption with Fenton pre-oxidation. J Hazard Mater 172:1131–1136

6. Chowdhary P, Bharagava RN, Mishra S, Khan N (2020) Role of industries in water scarcity and its adverse effects on environment and human health, Environmental concerns and sustainable development. Springer, pp 235–256
7. Cogal S, Celik Cogal G, Uygun Oksuz A (2021) Plasma-assisted synthesis of MnO2–polyaniline composite for electrochemical sensing of dopamine. Chem Pap 75:5163–5171
8. Crini G, Lichtfouse E (2019) Advantages and disadvantages of techniques used for wastewater treatment. Environ Chem Lett 17:145–155
9. Cuong DV, Wu P-C, Chen L-I, Hou C-H (2021) Active MnO2/biochar composite for efficient As (III) removal: Insight into the mechanisms of redox transformation and adsorption. Water Res 188:116495
10. Dong L, Zhu Z, Ma H, Qiu Y, Zhao J (2010) Simultaneous adsorption of lead and cadmium on MnO2-loaded resin. J Environ Sci 22:225–229
11. Elias E, Sarathchandran C, Joseph S, Zachariah AK, Thomas J, Devadasan D, Souza G Jr, Thomas F S (2021) Photoassisted degradation of rhodamine B using poly (ε-caprolactone) based nanocomposites: Mechanistic and kinetic features. J Appl Polym Sci 138:50612
12. Gangadharan D, Harshvardan K, Gnanasekar G, Dixit D, Popat KM, Anand PS (2010) Polymeric microspheres containing silver nanoparticles as a bactericidal agent for water disinfection. Water Res 44:5481–5487
13. Gangadharan D, Dixit D, Popat KM, Anand PS (2013) Amidoxime copolymer beads containing Cu/Cu2O microparticles as a biocidal material for water disinfection. J Appl Polym Sci 127:3491–3499
14. Georgin J, de O Salomón YL, Franco DS, Netto MS, Piccilli DG, Foletto EL, Dotto GL (2021) Successful adsorption of bright blue and methylene blue on modified pods of Caesalpinia echinata in discontinuous system. Environ Sci Pollut Res 28:8407–8420
15. Gürses A, Karaca S, Doğar Ç, Bayrak R, Açıkyıldız M, Yalçın M (2004) Determination of adsorptive properties of clay/water system: methylene blue sorption. J Colloid Interface Sci 269:310–314
16. Gürses A, Doğar Ç, Karaca S, Acikyildiz M, Bayrak R (2006) Production of granular activated carbon from waste Rosa canina sp. seeds and its adsorption characteristics for dye. J Hazard Mater 131:254–259
17. Han Q, Wang J, Goodman BA, Xie J, Liu Z (2020) High adsorption of methylene blue by activated carbon prepared from phosphoric acid treated eucalyptus residue. Powder Technol 366:239–248
18. Huang J-H, Huang K-L, Liu S-Q, Wang A-T, Yan C (2008) Adsorption of Rhodamine B and methyl orange on a hypercrosslinked polymeric adsorbent in aqueous solution. Colloids Surf A 330:55–61
19. Huang T, Yan M, He K, Huang Z, Zeng G, Chen A, Peng M, Li H, Yuan L, Chen G (2019) Efficient removal of methylene blue from aqueous solutions using magnetic graphene oxide modified zeolite. J Colloid Interface Sci 543:43–51
20. Hund-Rinke K, Simon M (2006) Ecotoxic effect of photocatalytic active nanoparticles (TiO2) on algae and daphnids (8 pp). Environ Sci Pollut Res 13:225–232
21. Joshiba GJ, Kumar PS, Govarthanan M, Ngueagni PT, Abilarasu A (2021) Investigation of magnetic silica nanocomposite immobilized Pseudomonas fluorescens as a biosorbent for the effective sequestration of Rhodamine B from aqueous systems. Environ Pollut 269:116173
22. Karthik G, Harith A, Thazleema NN, Vishal S, Jitha SJ, Saritha A (2018) : One step approach towards the green synthesis of silver decorated graphene nanocomposites for the degradation of organic dyes in water, IOP Conference Series: Materials Science and Engineering. IOP Publishing, pp. 012034

23. Khan TA, Dahiya S, Ali I (2012) Use of kaolinite as adsorbent: Equilibrium, dynamics and thermodynamic studies on the adsorption of Rhodamine B from aqueous solution. Appl Clay Sci 69:58–66
24. Khodakarami M, Bagheri M (2021) Recent advances in synthesis and application of polymer nanocomposites for water and wastewater treatment. J Clean Prod 296:126404
25. KK AV, Gangadharan D (2018) Valorisation of rhodamine B adsorbed copolymer beads for the recovery of Cu2 + from e-waste: Green approach. J Environ Chem Eng 6:7002–7009
26. KK AV, Gangadharan D (2022) Adsorptive remediation of organic pollutant and arsenic (V) ions from water using Fe3O4-MnO2 nanocomposite. Nano-Structures & Nano-Objects 29:100837
27. Kubra KT, Javaid A, Sharif R, Ali G, Iqbal F, Salman A, Shaheen F, Butt A, Iftikhar FJ (2020) Facile synthesis and electrochemical study of a ternary hybrid PANI/GNP/MnO2 as supercapacitor electrode material. J Mater Sci: Mater Electron 31:12455–12466
28. Kumar KV, Ramamurthi V, Sivanesan S (2005) Modeling the mechanism involved during the sorption of methylene blue onto fly ash. J Colloid Interface Sci 284:14–21
29. Li Y, Du Q, Liu T, Peng X, Wang J, Sun J, Wang Y, Wu S, Wang Z, Xia Y (2013) Comparative study of methylene blue dye adsorption onto activated carbon, graphene oxide, and carbon nanotubes. Chem Eng Res Des 91:361–368
30. Liu H, Ren X, Chen L (2016) Synthesis and characterization of magnetic metal–organic framework for the adsorptive removal of Rhodamine B from aqueous solution. J Ind Eng Chem 34:278–285
31. Liu L, Shen Z, Zhang X, Ma S (2019) Facile controlled synthesis of MnO2 nanostructures for high-performance anodes in lithium-ion batteries. J Mater Sci: Mater Electron 30:1480–1486
32. Nagarajan D, Venkatanarasimhan S (2019) Magnetite microparticles decorated cellulose sponge as an efficacious filter for improved arsenic (V) removal. J Environ Chem Eng 7:103386
33. Nagarajan D, Venkatanarasimhan S (2020) Kinetics and mechanism of efficient removal of Cu (II) ions from aqueous solutions using ethylenediamine functionalized cellulose sponge. Int J Biol Macromol 148:988–998
34. Namasivayam C, Sumithra S (2005) Removal of direct red 12B and methylene blue from water by adsorption onto Fe (III)/Cr (III) hydroxide, an industrial solid waste. J Environ Manage 74:207–215
35. Nhat Ha HN, Kim Phuong NT, Boi An T, Mai Tho NT, Ngoc Thang T, Quang Minh B, Van Du C (2016) Arsenate removal by layered double hydroxides embedded into spherical polymer beads: Batch and column studies. J Environ Sci Health Part A 51:403–413
36. Reddy DT, Shamini S, Ganesan V, Radhakrishnan A, Ajith V (2022) Intervention for improvement of water quality in a rural village in rajasthan, Smart Trends in Computing and Communications. Springer, pp 323–332
37. Sharma S, Hasan A, Kumar N, Pandey LM (2018) Removal of methylene blue dye from aqueous solution using immobilized Agrobacterium fabrum biomass along with iron oxide nanoparticles as biosorbent. Environ Sci Pollut Res 25:21605–21615
38. Skiba M, Vorobyova V (2020) Synthesis of Ag/TiO2 nanocomposite via plasma liquid interactions and degradation methylene blue. Appl Nanosci 10:4717–4723
39. Sureshkumar M, Namasivayam C (2008) Adsorption behavior of Direct Red 12B and Rhodamine B from water onto surfactant-modified coconut coir pith. Colloids Surf A 317:277–283
40. Tang AY, Lo CK, Kan C (2018) Textile dyes and human health: A systematic and citation network analysis review. Color Technol 134:245–257

41. Verma M, Tyagi I, Kumar V, Goel S, Vaya D, Kim H (2021) Fabrication of GO–MnO2 nanocomposite using hydrothermal process for cationic and anionic dyes adsorption: Kinetics, isotherm, and reusability. J Environ Chem Eng 9:106045
42. Xue H, Wang X, Xu Q, Dhaouadi F, Sellaoui L, Seliem MK, Lamine AB, Belmabrouk H, Bajahzar A, Bonilla-Petriciolet A (2022) Adsorption of methylene blue from aqueous solution on activated carbons and composite prepared from an agricultural waste biomass: A comparative study by experimental and advanced modeling analysis. Chem Eng J 430:132801
43. Zhang J, Zhu M, Jones I, Zhang Z, Gao J, Zhang D (2021) Performance of activated carbons prepared from spent tyres in the adsorption of rhodamine B in aqueous solutions. Environmental Science and Pollution Research, pp 1–11
44. Zhang X, Zhang P, Wu Z, Zhang L, Zeng G, Zhou C (2013) Adsorption of methylene blue onto humic acid-coated Fe3O4 nanoparticles. Colloids Surf A 435:85–90
45. Zhu Z, Xiang M, Li P, Shan L, Zhang P (2020) Surfactant-modified three-dimensional layered double hydroxide for the removal of methyl orange and rhodamine B: Extended investigations in binary dye systems. J Solid State Chem 288:121448

Figures

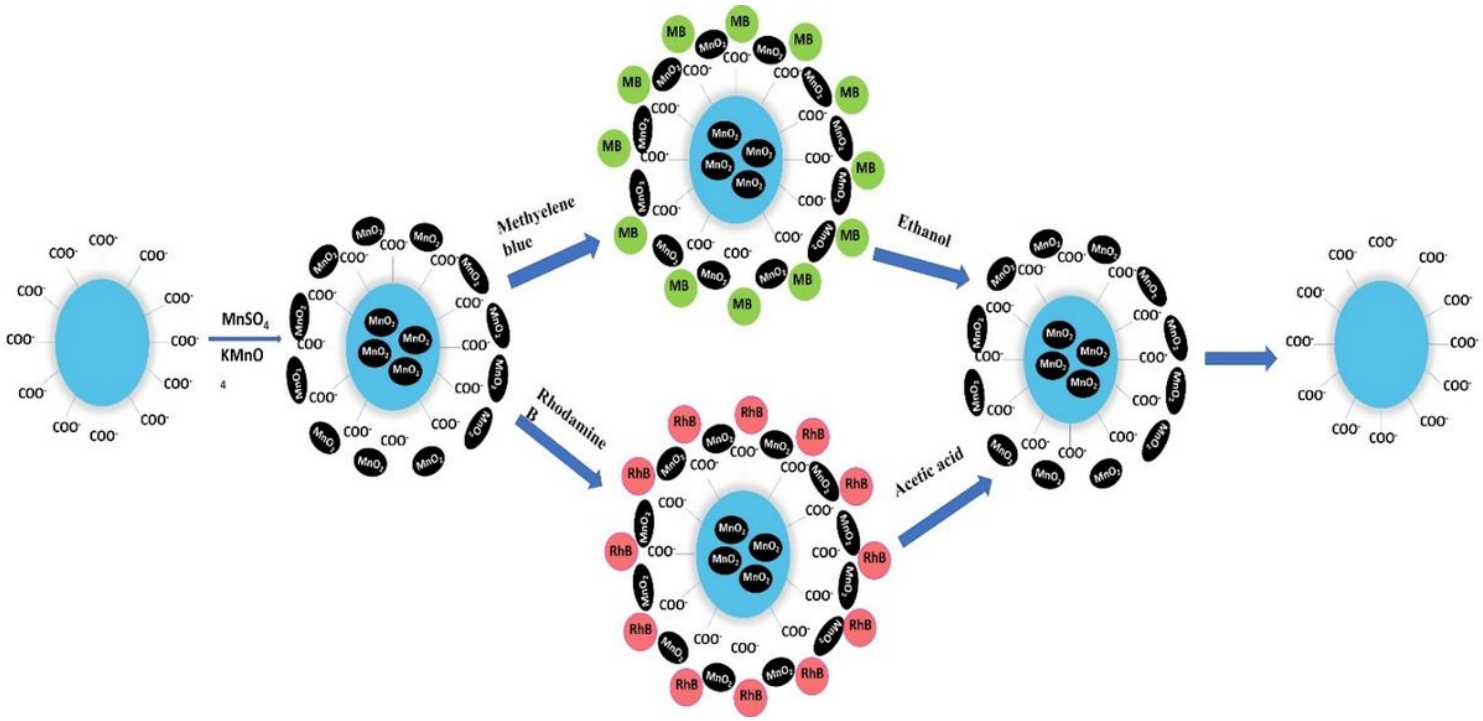

Figure 1

Scheme of work

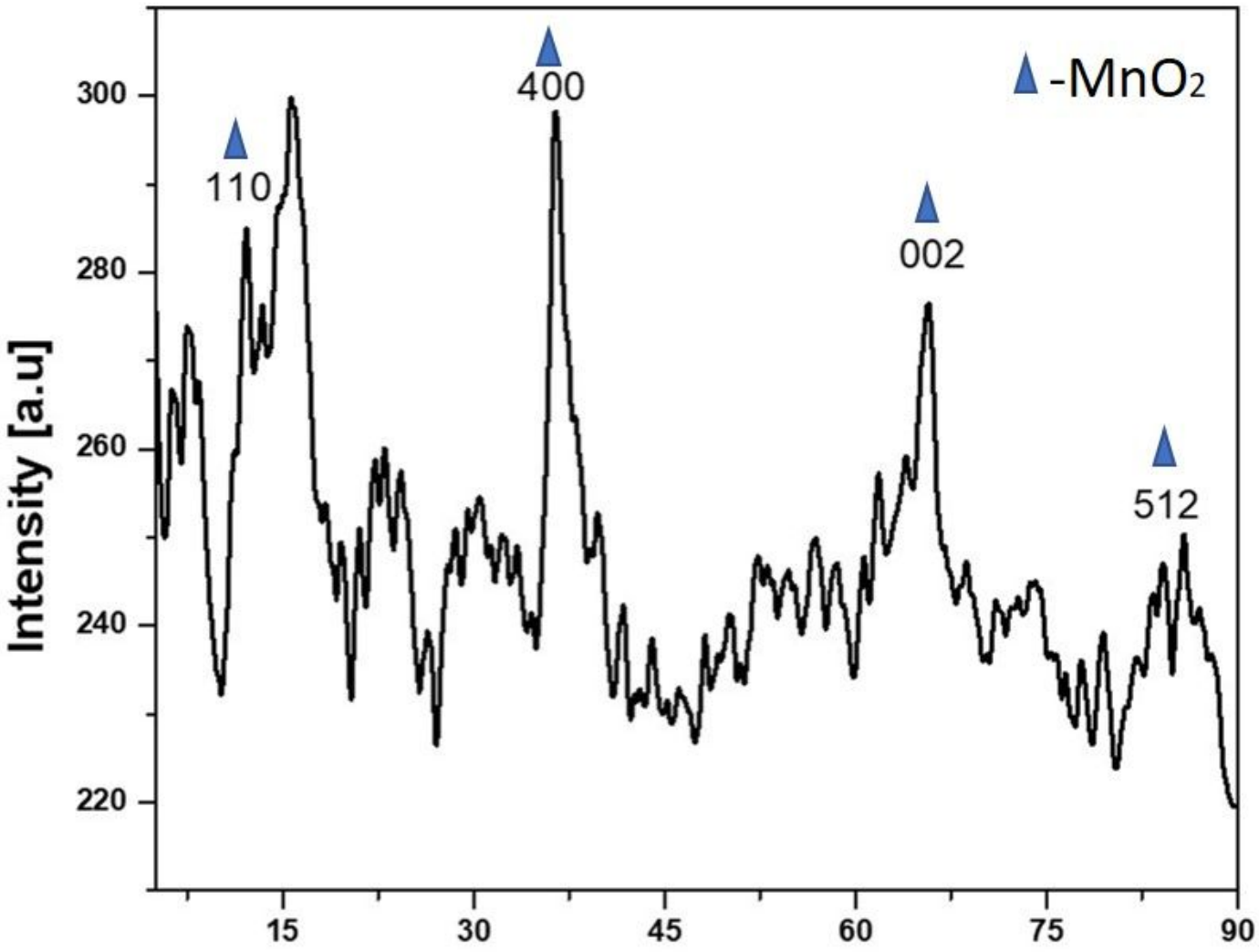

Figure 2

Powder X-ray diffraction pattern of copolymer-MnO_2 nanocomposite

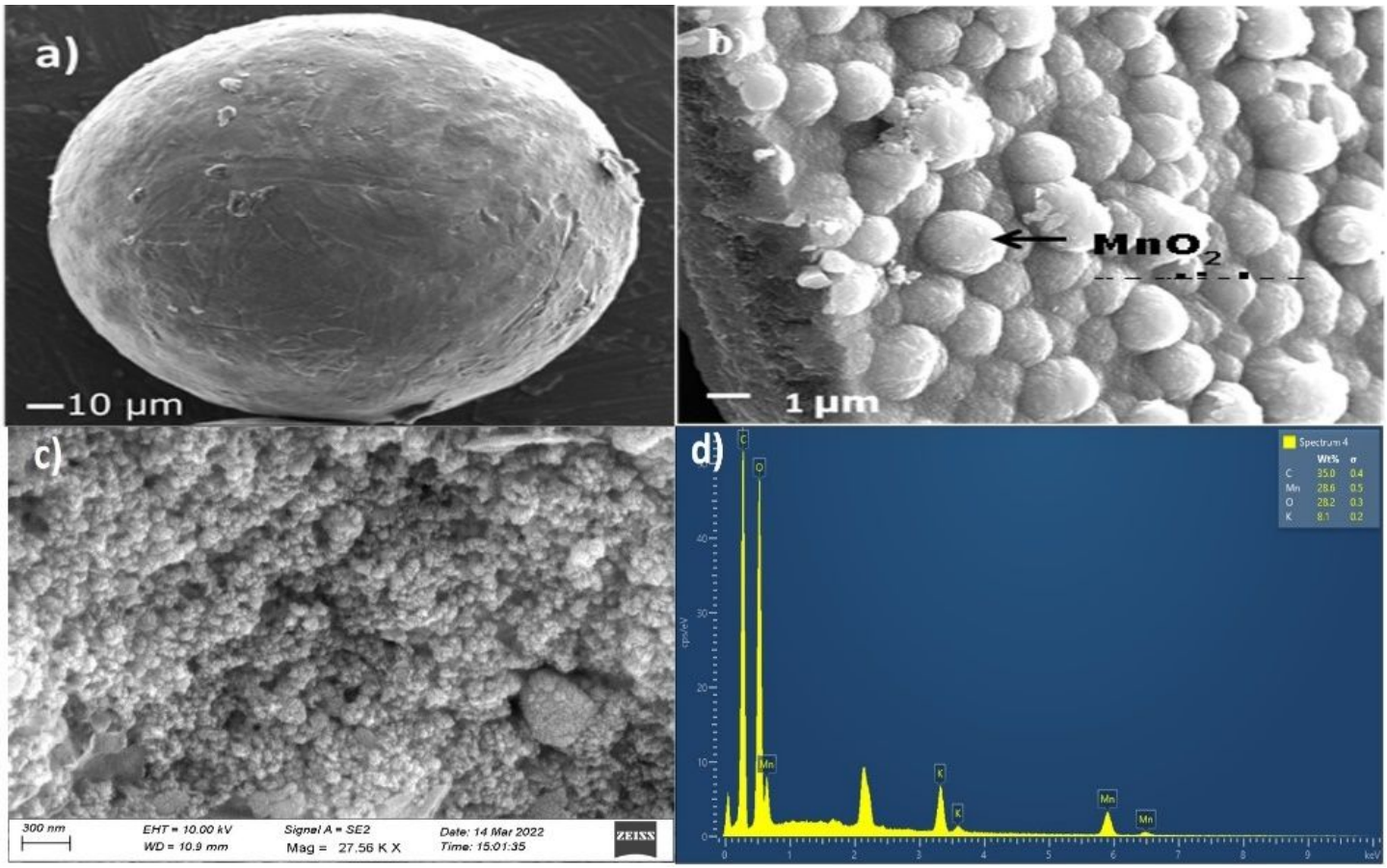

Figure 3

SEM images of a) polymer beads, and b) copolymer-MnO_2 nanocomposite.

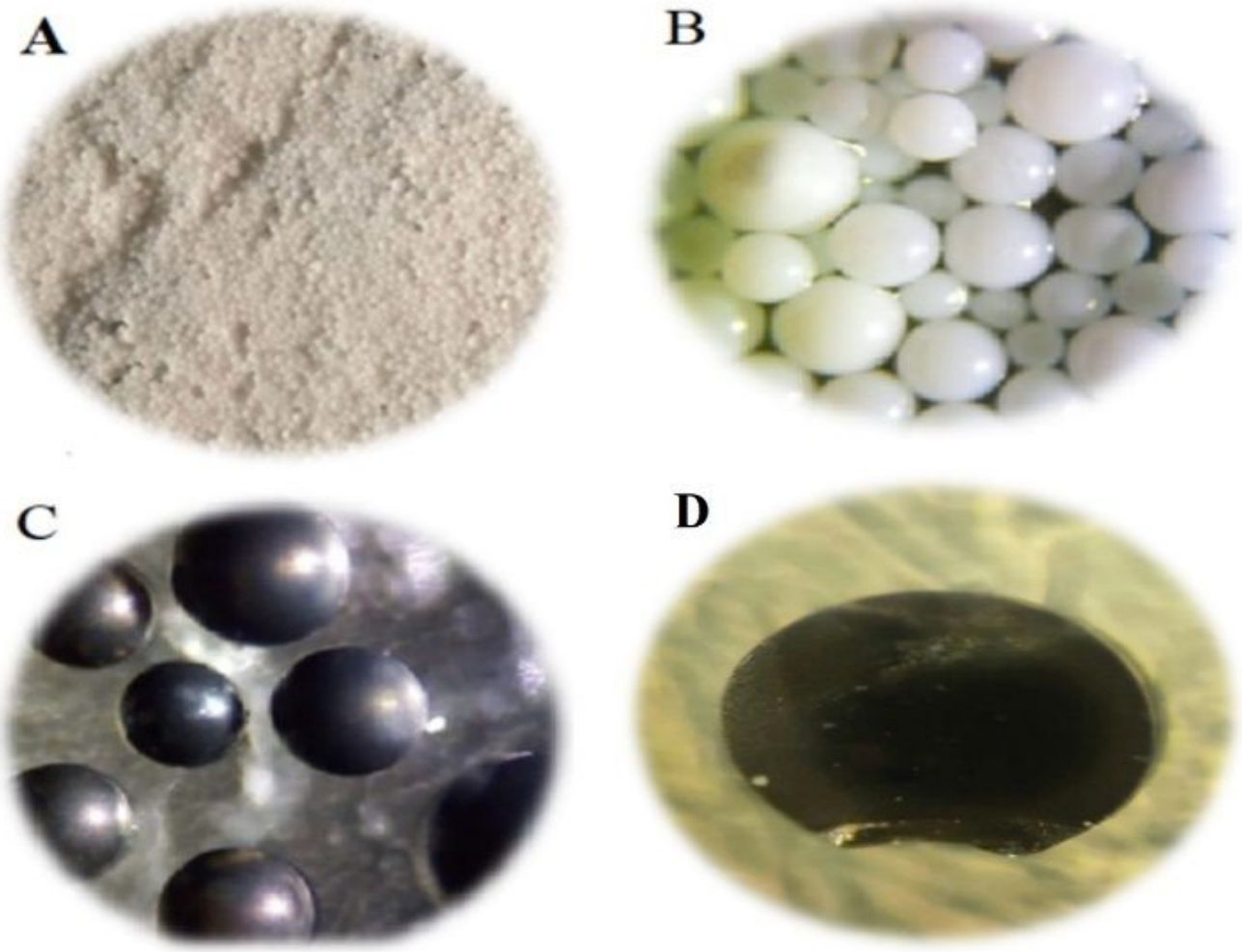

Figure 4

Microscopic images of a) The copolymer beads, b) Mn^{2+} loaded copolymer beads, c) copolymer-MnO_2 nanocomposite, d) cross section of the copolymer-MnO_2 nanocomposite.

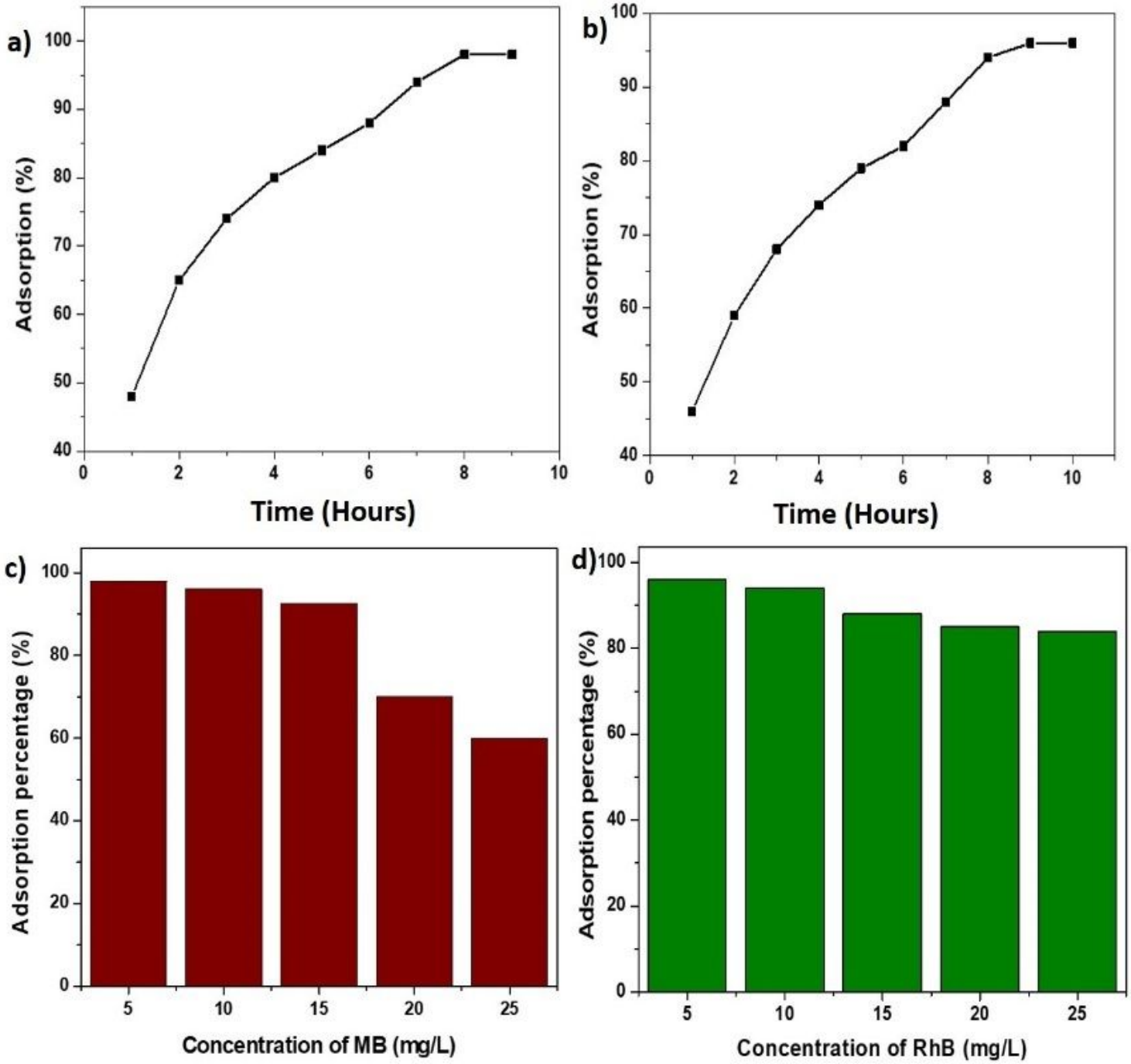

Figure 5

a) Adsorption of MB on copolymer-MnO_2 nanocomposite at different time interval b) adsorption of RhB on copolymer-MnO_2 nanocomposite at different time interval, c) Adsorption of MB from 5 to 25 mg/L concentration d) Adsorption of RhB from 5 to 25 mg/L concentration.

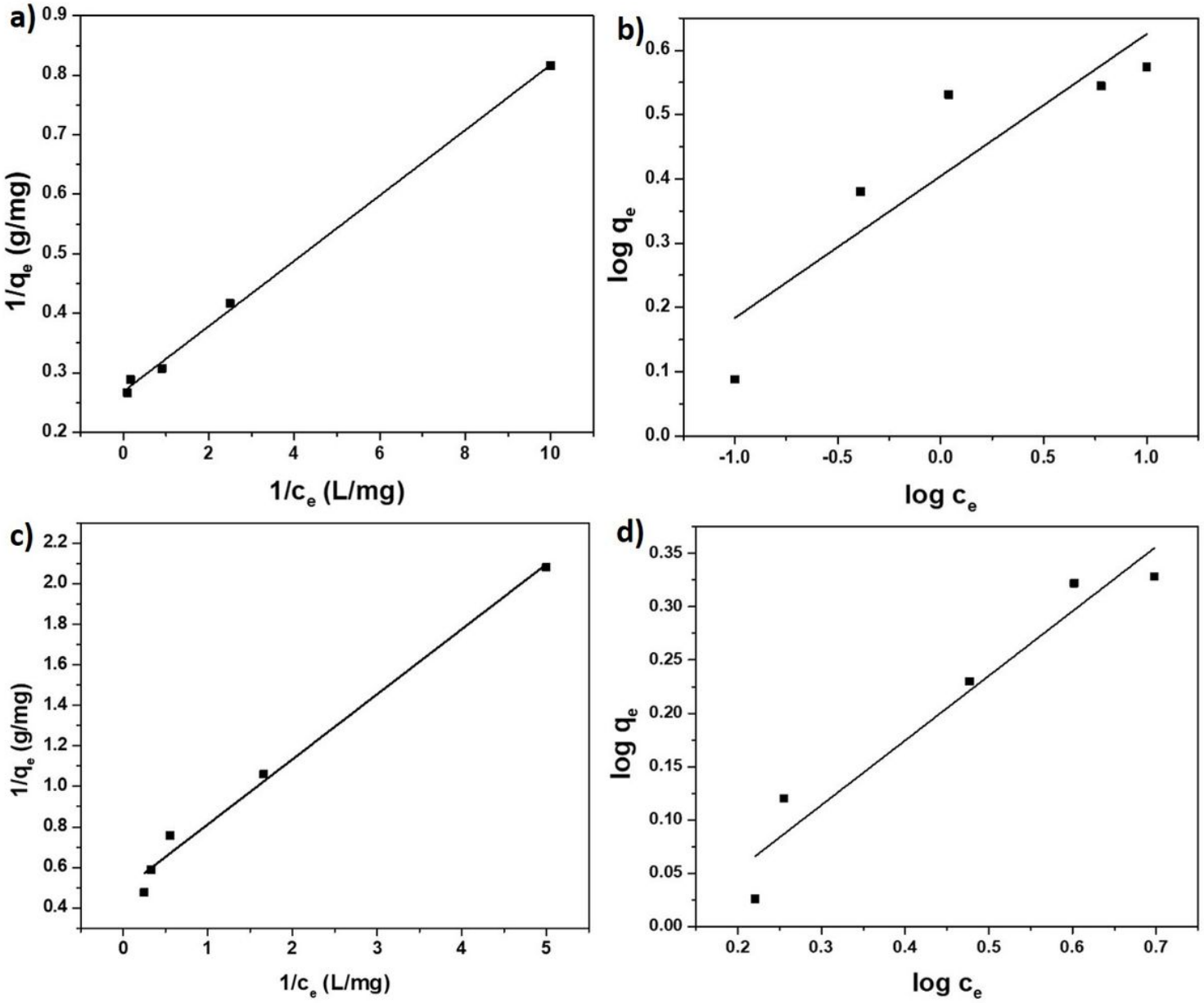

Figure 6

Linear fitting of Langmuir, and Freundlich isotherm for a) &b) adsorption of MB, and c) & d) for adsorption of RhB.

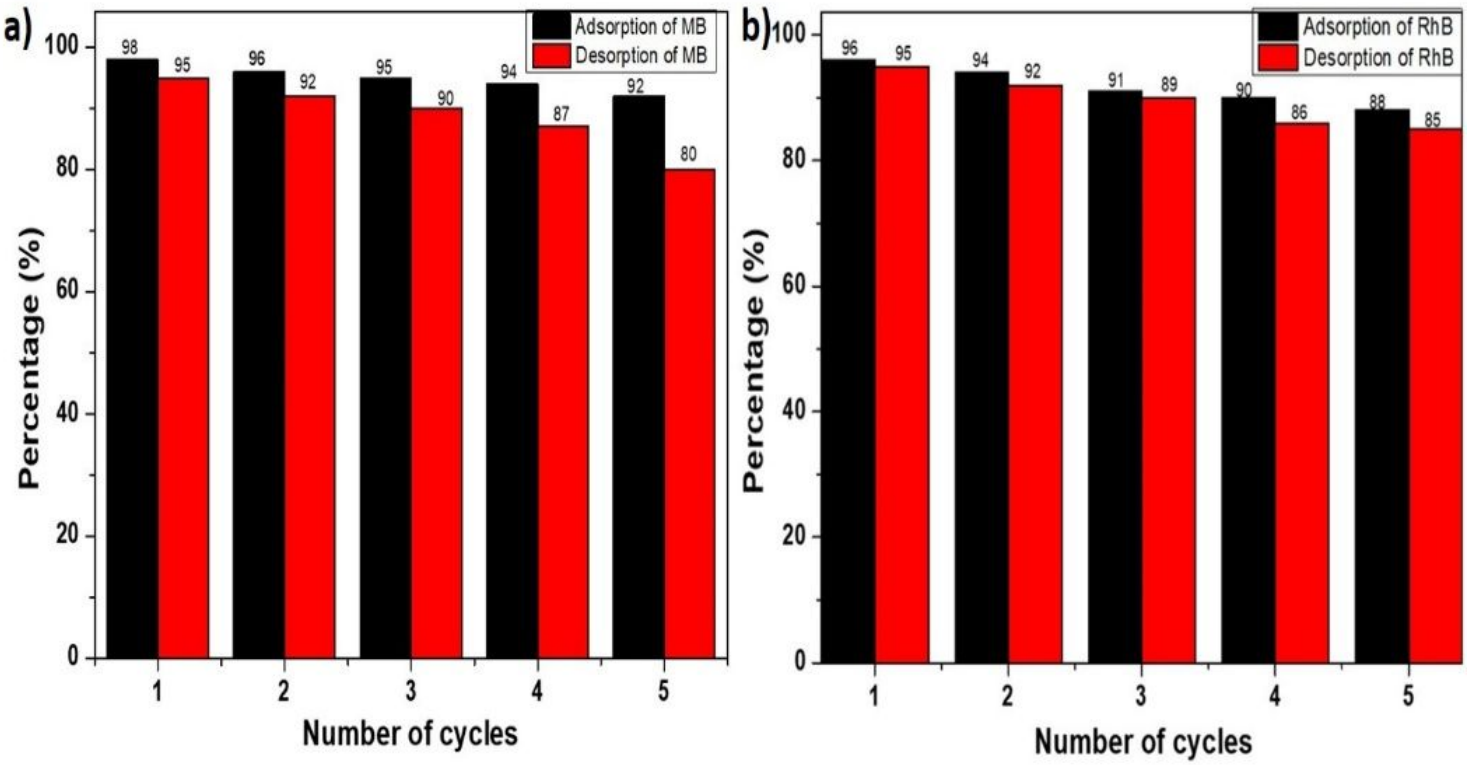

Figure 7

a) Percentage of MB adsorbed on copolymer-MnO_2 nanocomposite and percentage of MB desorbed from copolymer-MnO_2 nanocomposite b) percentage of RhB adsorbed on copolymer-MnO_2 nanocomposite, and percentage of RhB desorbed from copolymer-MnO_2 nanocomposite.

Supplementary Files

This is a list of supplementary files associated with this preprint. Click to download.

- GA.jpg